FATIGUE OF GLASS FIBRE REINFORCED POLYMERS FOR OCEAN ENERGY

C. R. Kennedy[a,c*], C. M. Ó Brádaigh[b,c], S. B. Leen[a,c]

[a]*Mechanical Engineering, NUI Galway, Ireland*
[b]*School of Engineering, University College Cork, Ireland*
[c]*Marine Renewable Energy Ireland (MaREI) Research Centre*
**ciaran.kennedy@nuigalway.ie*

Keywords: GFRP, Fatigue, Puck, Composite

Abstract

A combined experimental and computational study on the fatigue of glass-fibre reinforced polymers (GFRP) is presented, with particular emphasis on the effects of water saturation, for use in ocean energy structures. The experimental characterisation consisted (i) of immersion-aging of test specimens for a period of up to two years, using a moderate accelerated aging technique, designed to simulate longer-term seawater exposure of the material, and (ii) fatigue testing of aged and unaged specimens in immersed and non-immersed conditions, with emphasis on identification of fatigue damage evolution. The computational methodology incorporates the development of a multiaxial fatigue damage user material subroutine, based on the static Puck approach, adapted for fatigue by combining (i) fatigue-induced fibre strength and modulus degradation, (ii) irrecoverable cyclic strain effects and (iii) inter-fibre fatigue. Finally the impact of water saturation on the fatigue life of a tidal turbine blade is assessed using a fatigue life model.

1. Introduction

Glass fibre reinforced polymer materials are obvious candidates for use in marine renewable energy devices. Potential applications include tidal turbine blades, main structures and energy-collecting surfaces for wave energy devices and various nacelles, watertight compartments etc. In some of these applications a protective barrier (gel coat) between the water and the GFRP may be possible but it may suffer from either abrasion by sand or from surface cracking at strain levels likely to be experienced by marine renewable energy devices. Therefore it is conservative to assume that immersed GFRP may become moisture-saturated and its behaviour in this condition, under the fatigue loading expected with marine renewable energy devices, will be required in order to produce satisfactory designs for these machines.

2. Experimental method

2.1 Coupon manufacture

[(45°/135°/90°/0°)2]s laminates of epoxy / E-glass and vinyl ester / E-glass were fabricated using the VARTM (Vacuum Assisted Resin Transfer Moulding) process as described

elsewhere [1]. The laminates were oven cured at 80°C for approximately 4 hours. Fibre volume fractions of 50% were achieved at an average thickness of 3.75 mm.

2.2 Accelerated ageing procedure

Accelerated ageing has been used to simulate the effect of 20 years in cold (12°C) seawater by immersing the samples in warm (30°- 40°C) water for almost two years. For a higher temperature in the same material an acceleration factor based on the Arrhenius law of diffusion has been defined as [2]:

$$F_{H,L} = e^{\left[\frac{-E}{R}\left(\frac{1}{T_H}-\frac{1}{T_{ref}}\right)\right]} \quad (1)$$

Where *E* is the activation energy of the material, *R* is the universal gas constant (8.3145 kJ $kmol^{-1}K^{-1}$), *T* is the temperature in degrees Kelvin.

2.3 Fatigue test method

In general, the fatigue tests were carried out with an Instron 8001 test machine and 8800 controller, applying a sinusoidal force-time history in tension-tension mode (R = 0.1), at frequencies of between 3 and 6 Hz. At first, the wet coupons were just removed from the water and fatigue tested in the normal way. However it was realised that during high cycle fatigue testing (lasting a day or more) the coupons dry out due to the combination of internal heat generation and forced air cooling of the coupons. Allowing the coupons to dry out is not desirable as it has been shown [3] that epoxy and vinyl-ester composites recover most of their original strength when they are re-dried after water saturation. An approach using a water filled plastic pouch sealed with waterproof tape proved to be satisfactory and easy to implement as it allowed the use of the standard hydraulic jaws to grip the coupons.

3. Computational method

3.1 Fibre direction model

The degradation of fibre direction strength during fatigue cycling is assumed to follow the linear degradation per cycle suggested by Broutman and Sahu [4]. This has the advantage that only the expected life at each stress level is needed and this can be obtained from the SN curve or constant life diagram. A comparison of many candidate models recently concluded that the linear model was preferred based on its simplicity and conservative predictions [5].

The modulus of the material is also reduced as damage increases. True modulus is difficult to measure experimentally in fatigue testing and therefore secant modulus and fatigue modulus are used here instead. Fatigue modulus is defined here as the slope of a line which connects the minimum stress-strain point in a fatigue cycle with the maximum stress-strain point in the cycle. Mao and Mahadevan [6] have proposed the following equation to represent the typical s-shaped damage evolution of fatigue modulus with number of cycles

$$D = q\left(\frac{n}{N_f}\right)^{m1} + (1-q)\left(\frac{n}{N_f}\right)^{m2} \quad (2)$$

where *D* is the accumulated damage at n number of cycles, N_f is the fatigue life (number of cycles) at the load being applied and *q*, *m1*, *m2* are material dependent parameters.

Irrecoverable strain under fatigue loading with a tensile maximum load is also incorporated into this fatigue damage model. The approach adopted here is based on the assumption that the fibre direction irrecoverable strain increases in proportion to the change in fibre direction fatigue modulus.

3.2 Matrix governed model response

Puck has developed a criterion to predict static inter fibre failure based on lamina strengths in shear and under normal transverse stresses [7]. This static criterion has been modified here for use as a fatigue model, by replacing the static strengths with fatigue strength equivalents [8], for example:

$$f_E(\theta) = \sqrt{\left(\frac{\tau_{nt}}{R^A_{\perp\perp}(N)}\right)^2 + \left(\frac{\tau_{nl}}{R_{\perp\parallel}(N)}\right)^2 + \sigma_n^2\left(\frac{1}{R^{(+)}_{\perp}(N)} - \frac{p^{(+)}_{\perp\psi}}{R^A_{\perp\psi}(N)}\right)^2} + \frac{p^{(+)}_{\perp\psi}}{R^A_{\perp\psi}(N)}\sigma_n\,,\ for\ \sigma_n \geq 0 \quad (3)$$

where $f_E(\theta)$, called the stress exposure, is a measure of the fraction along the path to IFF. At stresses below IFF, $f_E(\theta)$ is less than 1.0; failure is predicted when $f_E(\theta)$ = 1. $R^A_{\perp\perp}(N)$ is the fatigue resistance to τ_{nt} (fibre rolling) shear stress, $R_{\perp\parallel}(N)$ is the fatigue resistance to τ_{nl} (fibre sliding) shear stress, $R^{(+)}_{\perp}(N)$ is the transverse tensile fatigue strength, $R^A_{\perp\psi}(N)R^{(-)}_{\perp}(N)$ is the combined fatigue shear resistance, and $p^{(+)}_{\perp\perp}\ p^{(-)}_{\perp\perp}\ p^{(+)}_{\perp\parallel}\ p^{(-)}_{\perp\parallel} p^{(\pm)}_{\perp\psi}$ is a parameter which controls the inclination of the failure envelope around zero transverse stress and has a recommended value of between 0.20 and 0.30 [9]. The matrix dominated moduli are degraded in a similar manner to the static model both before and after IFF based on the stress exposure level. As the fatigue strengths of the matrix are reduced with increasing fatigue cycles the stress exposure level will increase with a consequent decrease in the matrix moduli. The degradation in transverse tensile and compressive moduli before IFF is relatively small. After IFF the transverse tensile modulus undergoes rapid degradation as the cracks in the material separate whereas the transverse compressive modulus is unaffected as the cracks are pressed together. The shear modulus is treated similarly except in the case where the transverse stress is slightly compressive in which case the moderate degradation in shear modulus continues based on stress exposure.

3.3 FE laminate model

Figure 1 shows a unit cell model of a balanced, symmetric, quasi isotropic GFRP laminate ($[45/135/90/0]_s$) to mimic the experimental laminate. The model is a cube with 1.92 mm edge length and includes 8 plies with the material orientation in each ply specified in 45° increments. Each 0.240 mm thick ply has three 8-node brick elements through the thickness. Mesh convergence studies established this degree of mesh refinement to be sufficient for converged laminate stresses. The material behaviour including fatigue damage is implemented here and calibrated via a user material subroutine (UMAT) in the commercial FE code Abaqus. Symmetric boundary conditions are used on 3 faces to reduce modelling effort resulting in a 1/8th model of the laminate. This unit cell is assumed to be embedded in a large QI laminate which experiences uniaxial tensile loading.

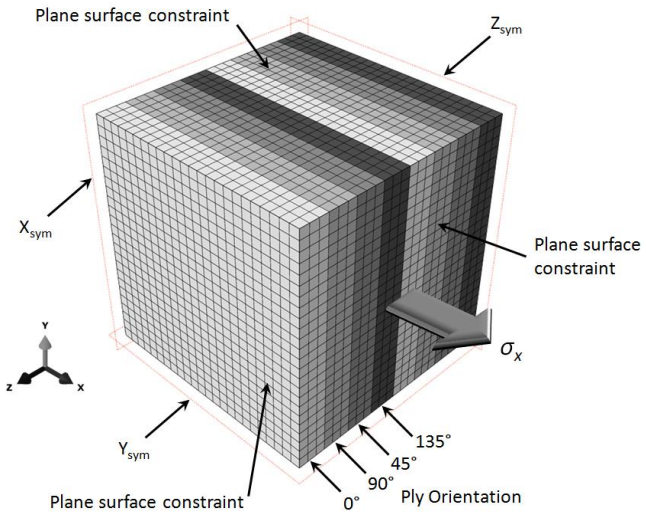

Figure 1. Unit cell model of $[45/135/90/0]_s$ epoxy / E-glass laminate.

Therefore it is assumed that all faces of the cube remain plane and this constraint is imposed on the 3 faces not constrained by symmetric boundary conditions. Initial damage to fibre direction modulus with a maximum level of 0.1% is randomly distributed in every element of the model.

3.4 Tidal turbine blade fatigue life model

A hydrodynamic-structural tidal blade analysis methodology [1] was used to predict the effect of water saturation on the fatigue life of a tidal turbine blade with a representational loading spectrum. Predictions were made for the fatigue life of both pitch-regulated and stall-regulated tidal turbine blades with dry and water saturated laminates.

4. Results

4.1 Water uptake during immersion ageing

Figure 2 shows the % weight of water absorbed by the epoxy / E-glass coupons while they were immersed in the ageing tanks at 30°C and at room temperature.

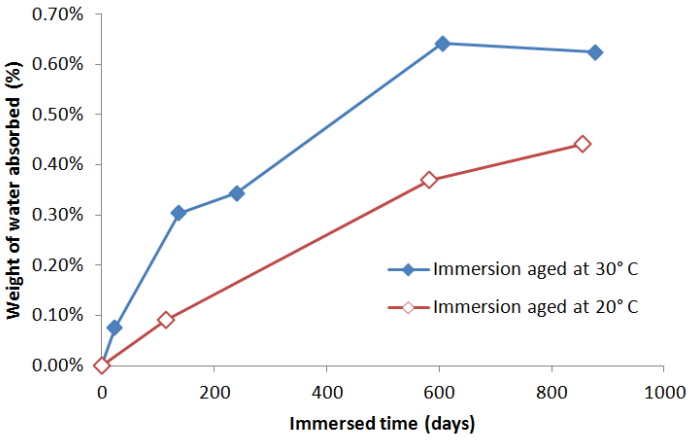

Figure 2. Weight of water absorbed by Epoxy / E-glass composite during water immersion ageing.

The increased diffusion activity stimulated by the higher temperature has enabled the coupons immersed in 30°C water to absorb water more quickly and become saturated at approximately 0.60% moisture. The coupons at room temperature absorbed water more slowly and had not become saturated by the end of the immersion period.

4.2 Fatigue stress-life curves

Figure 3 shows the results of fatigue testing epoxy / E-glass QI coupons in tension-tension mode (R = 0.1) for both the wet and dry coupons.

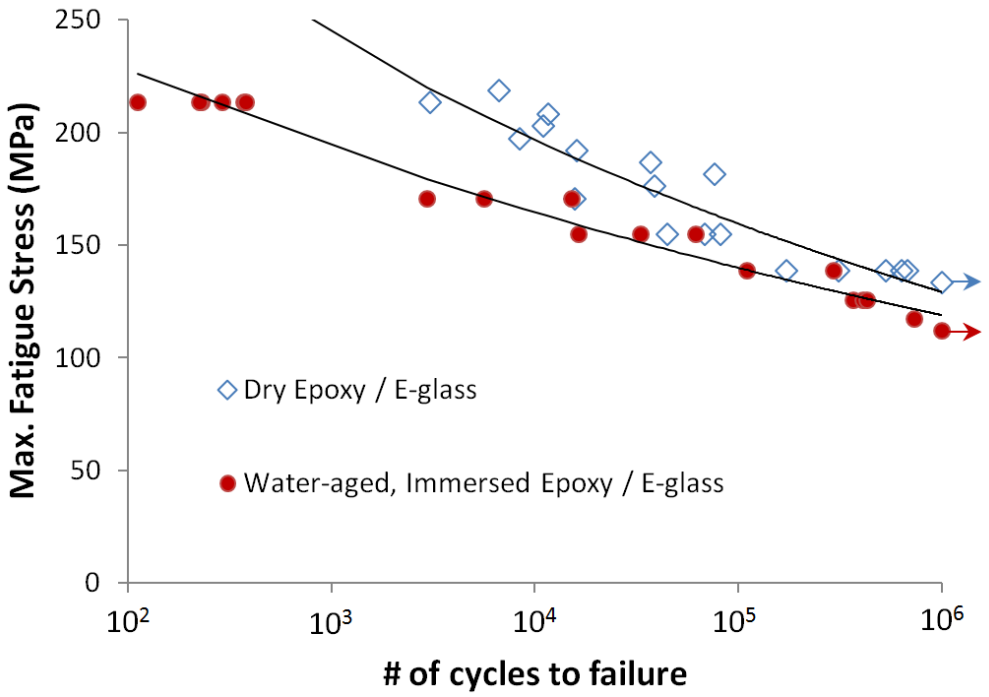

Figure 3. *Stress-life curves for wet and dry epoxy / E-glass in R = 0.1 fatigue tests.*

The results show a drop in fatigue strength for the water-aged, immersed coupons compared to the dry coupons which were tested in normal room temperature air. At high stresses the water-aged fatigue strength is 75% or 80% of the dry fatigue strength while at low stress (high cycles) the water-aged strength is about 90% of the fatigue strength of the dry material.

4.3 Stiffness degradation

The fatigue modulus was continuously monitored during the fatigue tests on both the dry and wet coupons. Figure 4 shows the evolution in fatigue modulus over the life of both wet and dry coupons at three different load levels. The graph shows that wet coupon stiffness decays in the same way as the dry coupons during fatigue cycling.

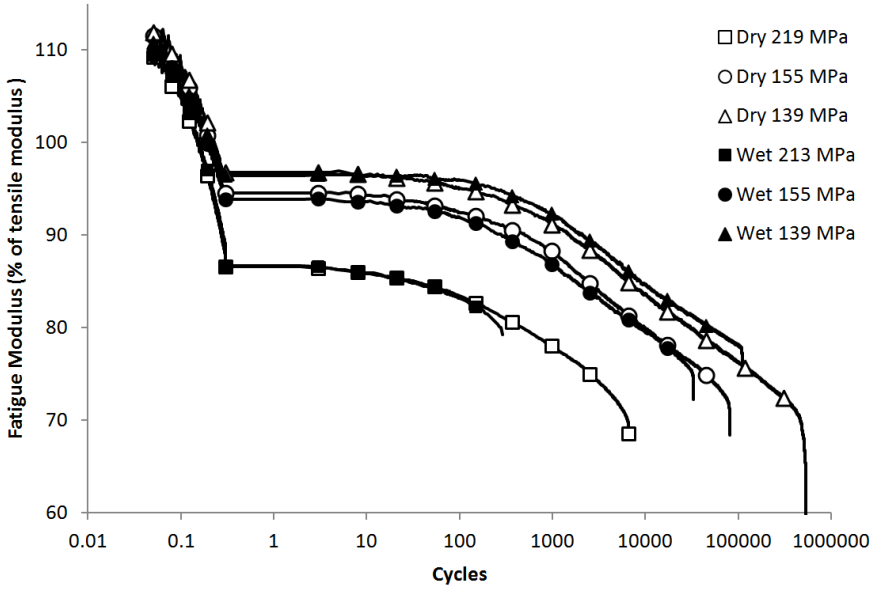

Figure 4. *Measured wet and dry modulus degradation during fatigue cycling at R = 0.1 of QI epoxy / E-glass.*

4.4 Predicted stiffness degradation

Figure 5 shows the measured evolution of fatigue modulus from a sample fatigue test at 155 MPa (maximum stress) compared to the predicted evolution (from the unit cell laminate model). Clearly the predicted response captures the overall modulus degradation in the first cycle and follows the evolution of degradation with subsequent cycles until failure at approximately 10^5 cycles.

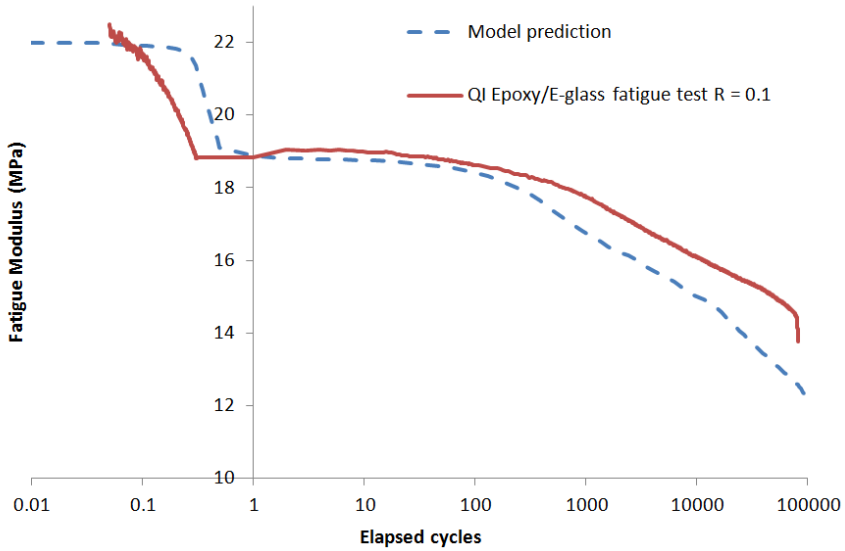

Figure 5. *Predicted and measured fatigue modulus during R = 0.1 fatigue testing of a QI epoxy / E-glass laminate at 155 MPa maximum stress.*

4.5 Predicted fatigue stress-life curves

Figure 6 shows the SN curves generated using damage model predictions of fatigue life for a range of constant amplitude fatigue stresses in both wet and dry quasi-isotropic epoxy / E-glass laminates. This model data is not graphically compared to the experimental data as there

are some differences in material makeup (fabric, epoxy type) and the fatigue strengths are therefore too different to make this comparison useful. However the model successfully predicts the stress dependence of the fatigue strength degradation due to water saturation and successfully captures the % difference between the wet and dry SN curves. At a fatigue life of 1,000 cycles, the prediction agrees with the experimental finding of a 20% reduction in fatigue strength due to water immersion. At 10^5 cycles fatigue life, the predicted fatigue strength reduction is 8% compared with a measured reduction of 12%.

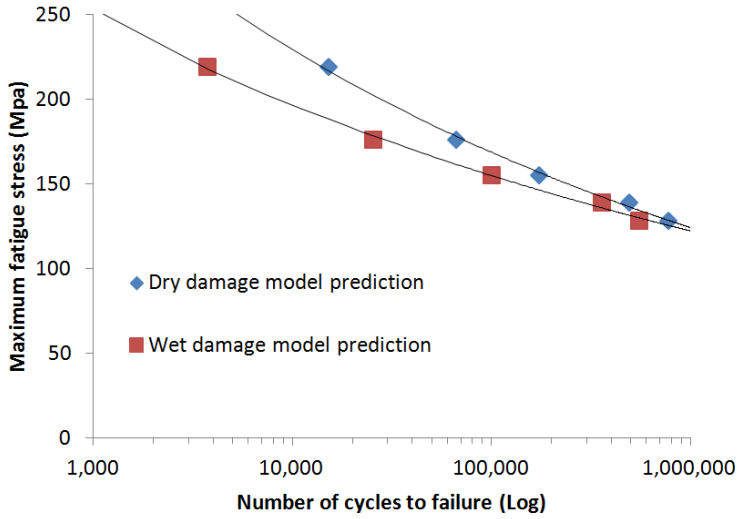

Figure 6. *Damage model predictions for wet and dry stress-life curves of QI epoxy / E-glass coupons in constant amplitude fatigue.*

4.6 Predicted reduction in tidal turbine blade life

Figure 7 shows that the predicted 20 year "dry" fatigue life of a stall-regulated tidal turbine blade is reduced to 17 years if the laminate is water saturated. Furthermore, if the maximum stress in the blade is 66 MPa, then the predicted "dry" life is 5 years and the predicted "wet" life is 2.9 years. For a pitch-regulated turbine blade the 20 year "dry" life is reduced to 19.1 years and the 5 year "dry" life is reduced to 3.3 years.

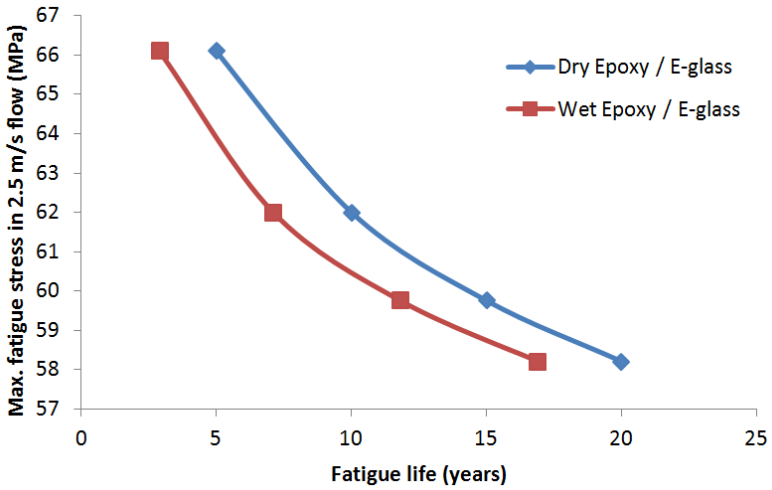

Figure 7. *Predicted effect of seawater immersion on fatigue life of stall-regulated tidal turbine blade (4.0 m/s max. tidal velocity).*

5. Conclusions

Experimental testing presented here shows that the fatigue strength of epoxy / E-glass coupons was significantly degraded by water immersion-ageing. For a fatigue life of 1,000 cycles, the wet fatigue strength is 20% less than the dry fatigue strength, whilst for a fatigue life of 1 million cycles, the wet fatigue strength is 8% less than the dry fatigue strength, so that the effect is also stress level dependent.

A ply level progressive damage model has been used to model both wet and dry laminate fatigue degradation under constant amplitude tensile (R = 0.1) fatigue stress. The model is shown to successfully predict knockdown factors for the effect of seawater immersion on the fatigue strength of QI epoxy / E-glass laminate across the range of fatigue lives. In particular the knockdown factor for 1,000 cycle fatigue life is equal (~20%) to that found experimentally and for 1×10^5 cycle fatigue life, the predicted knockdown factor is 8%, compared to the experimentally determined value of 12%.

The hydrodynamic-structural tidal blade analysis methodology with a cumulative damage model and a tidal turbine load spectrum was used to predict the fatigue life of tidal turbine blades. It showed that the maximum effect of water saturation is to reduce the 20-year predicted life of a stall-regulated blade by 15% and that of a pitch-regulated turbine blade by 4.5%.

References

[1] C. R. Kennedy, S. B. Leen, and C. M. Brádaigh, ‘A Preliminary Design Methodology for Fatigue Life Prediction of Polymer Composites for Tidal Turbine Blades’, *Proc. Inst. Mech. Eng. Part J. Mater. Des. Appl.*, vol. 226, no. 3, pp. 203–218, Jul. 2012.

[2] P. Purnell, J. Cain, P. van Itterbeeck, and J. Lesko, ‘Service life modelling of fibre composites: A unified approach’, *Compos. Sci. Technol.*, vol. 68, no. 15–16, pp. 3330–3336, Dec. 2008.

[3] P. Davies, F. MazEas, and P. Casari, ‘Sea Water Aging of Glass Reinforced Composites: Shear Behaviour and Damage Modelling’, *J. Compos. Mater.*, vol. 35, no. 15, pp. 1343–1372, Aug. 2001.

[4] Broutman, L.J and Sahu, S., ‘A New Theory to Predict Cumulative Fatigue Damage in Fiberglass Reinforced Plastics’, in *Composite Materials: Testing and Design (second conference)*, ASTM International, 1972.

[5] T. P. Philippidis and V. A. Passipoularidis, ‘Residual strength after fatigue in composites: Theory vs. experiment’, *Int. J. Fatigue*, vol. 29, no. 12, pp. 2104–2116, Dec. 2007.

[6] H. Mao and S. Mahadevan, ‘Fatigue damage modelling of composite materials’, *Compos. Struct.*, vol. 58, no. 4, pp. 405–410, Dec. 2002.

[7] A. Puck and M. Mannigel, ‘Physically based non-linear stress–strain relations for the inter-fibre fracture analysis of FRP laminates’, *Compos. Sci. Technol.*, vol. 67, no. 9, pp. 1955–1964, Jul. 2007.

[8] C. R. Kennedy, C. M. Ó. Brádaigh, and S. B. Leen, ‘A multiaxial fatigue damage model for fibre reinforced polymer composites’, *Compos. Struct.*, vol. 106, pp. 201–210, Dec. 2013.

[9] A. Puck, J. Kopp, and M. Knops, ‘Guidelines for the determination of the parameters in Puck’s action plane strength criterion’, *Compos. Sci. Technol.*, vol. 62, no. 3, pp. 371–378, Feb. 2002.